Quantifying the impact of ecological memory on the dynamics of interacting communities

Moein Khalighi[1*], Didier Gonze[2], Karoline Faust[3], Guilhem Sommeria-Klein[1], Leo Lahti[1*]

1 Department of Computing, Faculty of Technology, University of Turku, Finland

2 Unité de Chronobiologie Théorique, Faculté des Sciences CP 231, Université Libre de Bruxelles, Belgium

3 Laboratory of Molecular Bacteriology (Rega Institute), Department of Microbiology, Immunology and Transplantation, KU Leuven, Leuven, Belgium

* Corresponding authors

moein.khalighi@utu.fi (MKH)

leo.lahti@utu.fi (LL)

Abstract

Ecological memory refers to the influence of past events on the response of an ecosystem to exogenous or endogenous changes. Memory has been widely recognized as a key contributor to the dynamics of ecosystems and other complex systems, yet quantitative community models often ignore memory and its implications.

Recent studies have shown how interactions between community members can lead to the emergence of resilience and multistability under environmental perturbations. We demonstrate how memory can complement such models. We use the framework of fractional calculus to study how the outcomes of a well-characterized interaction model are affected by gradual increases in ecological memory under varying initial conditions, perturbations, and stochasticity.

Our results highlight the implications of memory on several key aspects of community dynamics. In general, memory slows down the overall dynamics and recovery times after perturbation, thus reducing the system's resilience. However, it simultaneously mitigates hysteresis and enhances the system's capacity to resist state shifts. Memory promotes long transient dynamics, such as long-standing oscillations and delayed regime shifts, and contributes to the emergence and persistence of alternative stable states.

Collectively, these results highlight the fundamental role of memory on ecological communities and provide new quantitative tools to analyse its impact under varying conditions.

Author summary

An ecosystem is said to exhibit *ecological memory* when its future states do not only depend on its current state but also on its initial state and trajectory. Memory may arise through various mechanisms as organisms learn from experience, modify their living environment, collect resources, and develop innovative strategies for competition and cooperation. Despite its commonness in nature, ecological memory and its potential influence on ecosystem dynamics have been so far overlooked in many applied contexts. Here, we combine theory and simulations to investigate how memory can influence community dynamics, stability, and composition. We incorporate in particular memory effects in a multi-species model recently introduced to investigate alternative stable states in microbial communities, and assess the impact of memory on key aspects of model behavior. The approach we propose for modeling memory has the potential to be more broadly applied in microbiome research, thus improving our understanding of microbial community dynamics and ultimately our ability to predict, manipulate and experimentally design microbial ecosystems.

Introduction

The temporal variations observed in ecosystems arise from the interplay of complex deterministic and stochastic processes, the identification and characterization of which requires quantitative models. The empirical study of microbial communities provides an ideal source of data to inform the development of dynamical community models, since this active research area generates rich ecological time series under highly controlled experimental conditions and perturbations [1]. Nevertheless, despite the recent advances in metagenomic sequencing and other high-throughput profiling technologies that are now transforming the analysis of microbial communities [2], there has only been limited success in accurately modeling and predicting the complex dynamics in microbial communities. This highlights the need for re-evaluating and extending the available models to better account for the various mechanisms that underlie community dynamics [1,3–7]. One central shortcoming of the currently popular dynamical models is that they ignore the role of memory, that is, they are based on the assumption that the community's future behavior solely depends on its current state, perturbations, and stochasticity.

Ecological memory is present when the community's past states and trajectories influence its dynamics over extended periods. It is a fundamental aspect of natural communities, and its influence on community dynamics has been widely recognized across ecological systems [8–11]. Memory can emerge through a

number of mechanisms, including the accumulation of abiotic and biotic material characterizing past legacies of the system [12, 13]. Thus, developing and investigating new means to incorporate memory in dynamical models of ecological communities has the potential to yield more accurate mechanistic understanding and predictions.

Diverse approaches have been proposed to explore ecological memory, including time delays [10, 14, 15], historical effects [16], exogenous memory [11], and buffering of disturbances [17]. A stochastic framework was used to evaluate the length, patterns, and strength of memory in ecological case studies [10]. However, the impact of memory has not been systematically addressed, and specific methods have been missing for incorporating memory into standard deterministic models of microbial community dynamics.

Potential community assembly mechanisms have been recently investigated based on extensions of the generalized Lotka-Volterra framework, which provides a standard model for species interactions [18–20]. The standard model has been extended by incorporating external perturbations [21], sequencing noise [22] and variance components [23], and to satisfy specific modeling constraints [24] such as compositionality [25]. Generalized Lotka-Volterra models have also been combined with Bayesian Networks for improved longitudinal predictions [26]. One goal of these modeling efforts is to understand how the alternative community types reported in the human microbiome may arise, possibly in combination with external factors [27–31]. Despite the recent popularity of generalized Lotka-Volterra models in microbial ecology, the impact of memory in these models has been largely ignored.

We address the above shortcomings by explicitly incorporating a class of memory effects into community interaction models using fractional calculus, which provides well-established tools for modeling memory [32, 33]. We incorporate memory into a multi-species model that was recently used to illustrate the emergence of alternative states in microbial communities [18], and we then use this extended model to demonstrate how memory can influence critical aspects of community dynamics. This contributes to the growing body of quantitative techniques for studying community resistance, resilience, prolonged instability, transient dynamics, and abrupt regime shifts [34–38].

Model

The generalized Lotka-Volterra and its extensions are ordinary differential equation (ODE) systems. This class of models has been commonly used to model community dynamics, but their standard formulations ignore memory effects. Here, we show how ecological memory can be included in these models based on *fractional calculus*. This mathematical tool provides a principled framework for incorporating memory effects into ODE systems (see *e.g.* [32, 33, 39, 40]), thus allowing a systematic analysis and quantification of memory effects in commonly used dynamical models of ecological communities.

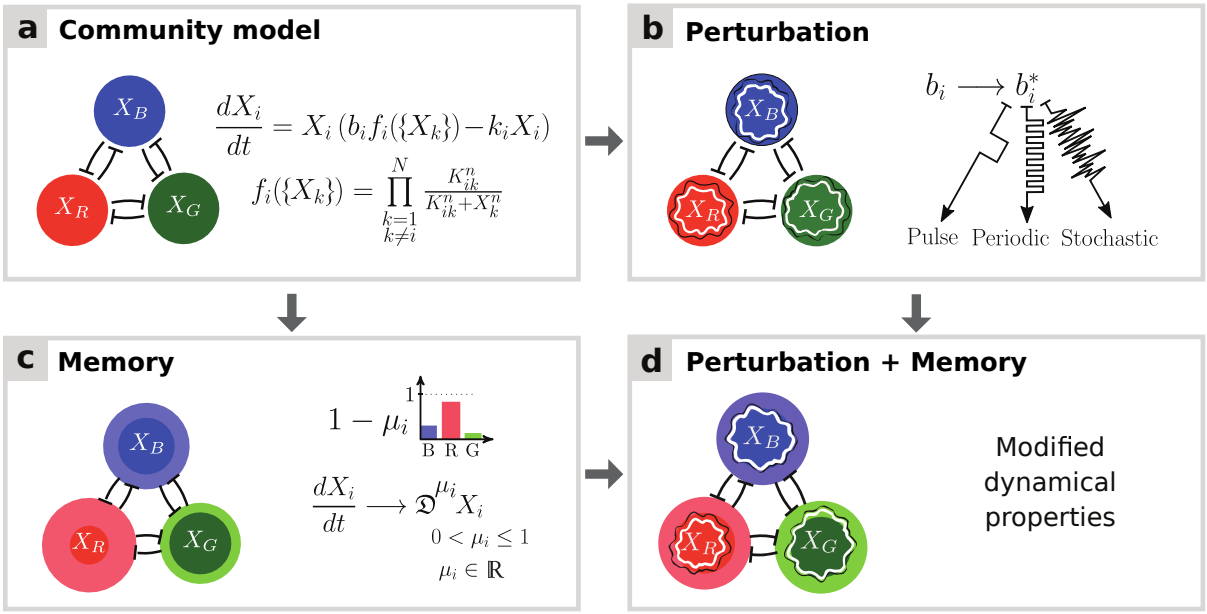

Fig 1. Schematic illustration of a three-species community in the presence of memory and perturbations. **(a)** The mutual interaction model describes the dynamics of species abundances X_i, which depends on the growth rates b_i, death rates k_i, and inhibition functions f_i, where K_{ij} and n denote interaction constants and Hill coefficients, respectively [18]. **(b)** Standard perturbations include pulse, periodic, and stochastic variation in species immigration, death, or growth rates. Such perturbations may trigger shifts between alternative states. **(c)** Memory (bolded circles) can be incorporated into dynamical models by substituting the integer-order derivatives with fractional derivatives $\mathfrak{D}^{\mu_i}$ of order μ_i (see [32] and Appendix S1). As decreasing μ_i values correspond to increasing memory, memory is measured as $1 - \mu_i$. When all community members have the same memory ($\mu_i = \mu$ for all i), the system is said to have *commensurate* memory, otherwise *incommensurate*. Increasing memory changes community dynamics, in particular by slowing it down and modifying the stability landscape around stable states. **(d)** Ecological memory can change the system's dynamics under perturbation.

Let us first consider a simple community with three species that tend to inhibit each other's growth (Fig 1a). We will later extend this model community to a larger number of species. To model this system, we employ a non-linear extension of the generalized Lotka-Volterra model that was recently used to demonstrate possible mechanisms underlying the emergence of alternative states in a multi-species community [18]. This non-linear model describes the dynamics of a species i as a function of its growth rate, death rate, and an interaction term determined by the interaction matrix between all species pairs, as described in Fig 1a. Under certain conditions, this model gives rise to a tristable community, where each stable state corresponds to the dominance of a different species. The community can shift from one stable state to another following an external or internal perturbation (Fig 1b).

To introduce memory, we extend this model by incorporating fractional derivatives. In this extended formulation, the classical derivative operator d/dt is replaced by the fractional derivative operator $\mathfrak{D}^{\mu_i}$, where $\mu_i \in]0, 1]$ is the non-integer derivative order for species i (Fig 1c). The fractional derivative is defined by a convolution integral with a power-law memory kernel (see Appendix S1). The μ_i can then be used as a tuning parameter for memory, with lower values of μ_i indicating higher levels of memory for

species i [32]. The *strength of memory* for species i is measured as $1 - \mu_i$. The three special cases of this model include (i) *no memory* ($\mu_i = \mu = 1$ for all species i), which corresponds to the original community model in [18]; (ii) *commensurate memory*, where all species have equal memory ($\mu_i = \mu \leq 1$); and (iii) *incommensurate memory*, where μ_i may be unique for each i, and hence the degree of memory may differ between species. We numerically solve the fractional-order model with varying values of the parameter μ_i, thus inducing varying levels of memory, and use it to analyse the effect of memory on various aspects of community dynamics, in particular its response to perturbations (Fig 1d).

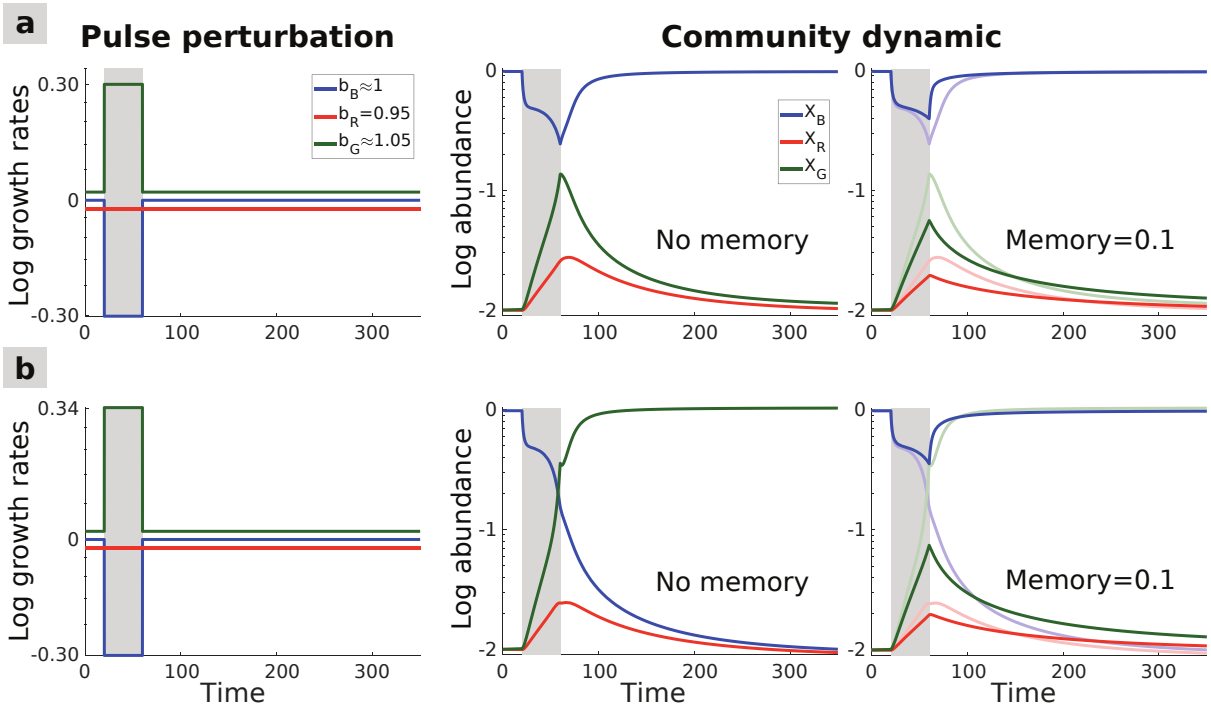

Fig 2. Impact of commensurate memory on community resistance and resilience. (a) A pulse perturbation is applied to the community (left panel): the growth rate of the blue species is lowered while that of the green species is simultaneously raised. The perturbation temporarily moves the community away from its initial stable state, characterized by blue species dominance (middle panel). Introducing commensurate memory (right panel) increases resistance to perturbation since the community is not displaced as far from its initial state compared to the memoryless case (shown in superimposition). The effect on resilience depends on the time scale considered: while memory initially hastens the recovery after the perturbation, it slows down the later stages of the recovery (starting around the time step 150). **(b)** A slightly stronger pulse perturbation is applied (left panel), triggering a shift toward an alternative stable state dominated by the green species (middle panel). Memory can prevent the state shift (right panel). Thus, here, not only does memory increase community resistance to perturbation, but also resilience as manifested by the prevented state shift.

Results

We have shown above how ecological memory can be incorporated in dynamical community models based on the framework of fractional calculus. Next, we use numerical simulations and analyses of this model to highlight the impact of memory on key dynamical properties of multi-species communities.

In general, memory adds a certain inertia in community dynamics as the influence of past states gradually fades out. Commensurate memory thus slows down the overall dynamics, which may lead to qualitative changes in the dynamics as well as community composition under certain conditions. In particular, memory-induced inertia tends to damp down fluctuations and can therefore mitigate or prevent more extreme and sudden changes in the system. Overall, our results show that ecological memory affects the community dynamics in two important ways: by enforcing more moderate levels of fluctuations, and by inducing quantitative and qualitative changes in how the system responds to perturbations or varying initial conditions. In the first section below, we report the consequences of these changes on community resistance and resilience.

The emergence of alternative community states has been debated in the microbiome research literature. For instance, [18] demonstrated how pulse perturbations can bring the 3-species system to a boundary of the tristability region, which then triggers a transition to an alternative stable state. In that model, such a transition can be for instance controlled by changes in the species' growth rates. In the second section below, we report how memory can exert additional influence on the resulting dynamics and alter the community's stability landscape.

Resistance and resilience

Resistance refers to a system's capacity to withstand a perturbation without changing its state, while *resilience* refers to its capacity to recover to its original state after a perturbation [41]. To examine the impact of ecological memory on community resistance and resilience in response to perturbations, we perturbed the system by changing the species growth rates over time. Specifically, we investigated the three-species community under *pulse* (Figs 2), *periodic* (Fig 3), and *stochastic* (Figs 4) perturbations, and analysed the impact of these three types of perturbations on community dynamics in the presence of memory, which is commensurate in this subsection.

Our results show that memory tends to increase resistance to perturbations by allowing the competing species' coexistence for a longer time. In the presence of memory, switches between alternative community states take place more slowly following a pulse perturbation (Fig 2a), or in some cases may be prevented entirely (Fig 2b). Fig S1 provides a further example of the increased resistance provided by memory in a larger, unstructured community, where memory helps preserve the stable state after a pulse perturbation compared to the corresponding memoryless system.

After the perturbation has ceased, memory initially hastens the return to the original state, but then slows it down in the later stages of the recovery (Fig 2a). Thus, the impact of memory on resilience is multi-faceted: depending on the time scale considered, memory may either slow down or hasten the recovery from perturbations, thus reducing or increasing resilience. Furthermore, in multistable systems,

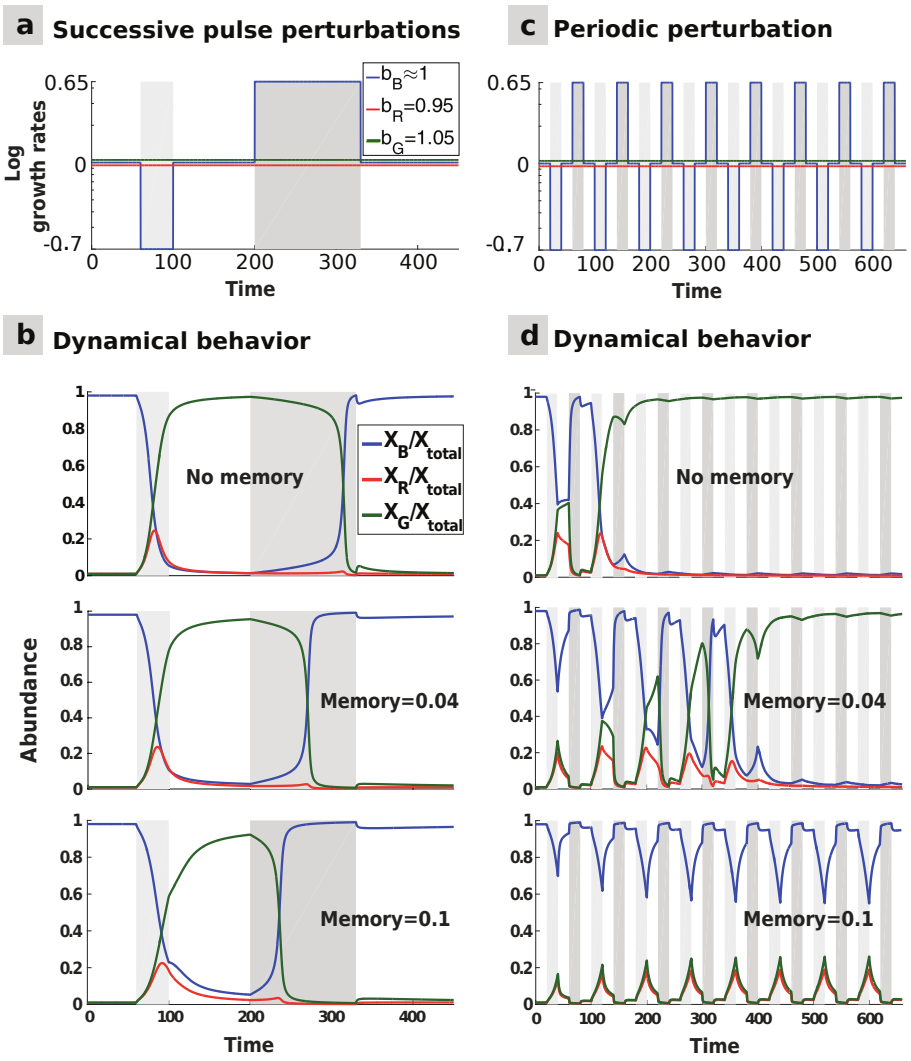

Fig 3. Multi-pulse and periodic perturbations: memory impact on hysteresis and transient oscillations. **(a)** Two opposite pulse perturbations are applied successively: the blue species growth rate is first briefly lowered, and then raised for a longer time. **(b)** The top panel shows the hysteresis in the system: the state shift towards the dominance of the green species occurs faster after the first perturbation than the shift back to the initial stable state after the second perturbation. Introducing commensurate memory (middle and bottom panels) delays the first state shift, thus increasing resistance, and hastens the second state shift, thus mitigating the hysteresis effect and increasing long-term resilience. **(c)** Rapidly alternating opposite perturbations are applied to the blue species growth rate with a regular frequency. **(d)** Without memory (top), the hysteresis effect leads to a permanent shift towards the green-dominated alternative stable state after a few oscillations. Adding commensurate memory mitigates the hysteresis, thus extending the transitory period (middle), which may generate longstanding oscillations in community composition before the community converges to a stable state (bottom).

memory may enhance resilience by promoting the persistence of the original stable state (Fig 2b).

Considering two successive pulse perturbations in opposite directions highlights another way memory can affect resilience in multistable systems (Fig 3a). After a state shift triggered by a first perturbation, memory may hasten recovery to the initial state following a second, opposite perturbation, hence increasing long-term resilience. Memory can thus mitigate the hysteresis that is typical of many ecological systems.

In the presence of regularly alternating opposite pulse perturbations, akin to those experienced by marine plankton or the gut microbiome, the community may not be able to recover its initial state if the perturbations follow each other too rapidly. In such circumstances, memoryless communities reach a new stable state faster than the communities with memory, as the latter resist the perturbations for a longer time due to the reduced hysteresis (Fig 3b). This may lead to community dynamics being trapped in long-lasting transient oscillations.

Finally, we analyse the role of stochastic perturbations, which are an essential component of variation in real systems. Under stochastic perturbation (Fig 4a), ecological memory can dampen the fluctuations and significantly delay the shift towards an alternative stable state (Fig 4b). This demonstrates in a more realistic perturbation setting how memory can promote community resistance.

Memory can nevertheless have unexpected effects on community dynamics when its strength is tuned to bring the system in the vicinity of the tristable region, where the outcome of the dynamics is highly sensitive to initial conditions (Fig 4c). Under such conditions, minute changes in memory can push the system over a tipping point towards another attractor, radically changing the outcome. This illustrates that, beyond slowing down the dynamics and damping perturbations, memory can have non-trivial effects on the system's stability landscape, which we investigate in the next section.

Impact on stability landscape

Let us now consider a more complex community of 15 species structured into three groups through their interaction matrix. Each of these groups represents a set of weakly competing species—*e.g.*, due to cross-feeding interactions that mitigate competition, while species belonging to different groups compete more strongly with each other (Fig 5a). We show that adding incommensurate memory in such a system can change the final stable state of the community even in the absence of perturbation. In particular, increasing the strength of memory in the group that is dominant in the stable state of the memoryless system can lead to its exclusion from the new stable state (Fig 5b-c). Around the threshold value, long transients can be observed (Fig 5d): even without changing any of the model parameters or imposing noise, an abrupt regime shift is triggered by the accumulated effect of memory after a long period of subtle, gradual changes.

Remarkably, adding memory in a given species may lead to either a reduction or an increase in its

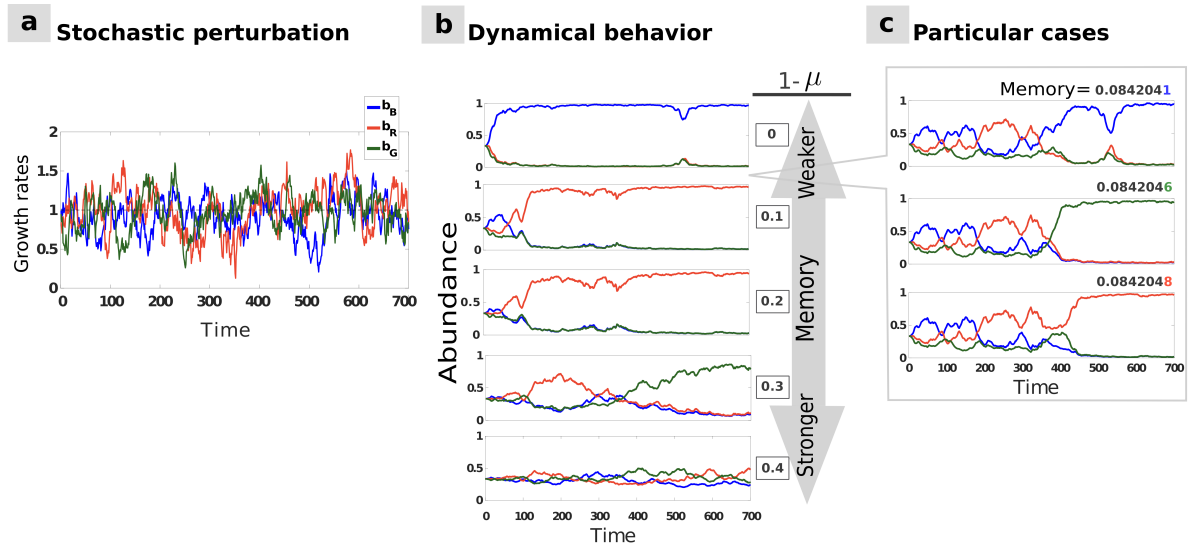

Fig 4. Stochastic perturbations with commensurate memory effects. **(a)** Stochastic perturbation in a three-species system: species growth rates b_i vary stochastically through time according to an Ornstein-Uhlenbeck process (see Appendix S2). **(b)** Dynamical behavior of the system in response to the stochastic perturbation for equal initial species abundances and varying memory level: in addition to slowing down community dynamics, increasing memory limits the overall variation in species abundances, thus enhancing the overall resistance of the system. **(c)** For some memory strengths, the final state of the system can be sensitive to slight variations in memory, with drastic consequences on community composition.

abundance depending on the conditions. While Fig 5b-c illustrates the exclusion of a group of species with higher memory from the stable state in the absence of perturbation, memory may conversely increase the persistence or abundance of a species in the presence of stochastic perturbation (Fig S2b). In fact, in the presence of perturbation, the dominance of any of the species may be achieved by tuning memory in a single species. This result holds both in the case of pulse (Fig S2a) and stochastic (Fig S2b) perturbation.

Bifurcation diagrams further show that, in addition to modifying the boundary between stable states in the space of initial conditions, memory can also broaden the region of the model's parameter space that exhibits multistability (Fig S3). We illustrate for instance in Figure 6 that incommensurate memory can induce multistability in a 3-species community that would otherwise converge to a single stable state in the absence of memory. Ecological memory thus provides an alternative and largely overlooked mechanism for the emergence of multistability.

Finally, we show that simply setting similar levels of ecological memory within groups of species in an otherwise unstructured community may lead to the formation of coherent species assemblages with shared dynamics (Fig S4). This provides an additional mechanism for the emergence of distinct community types, each associated with the dominance of one such assemblage. Hence, our results show that memory can by itself lead to the emergence of alternative community types, between which the community may switch following a change in either initial conditions (Fig 6) or memory strength (Fig S4).

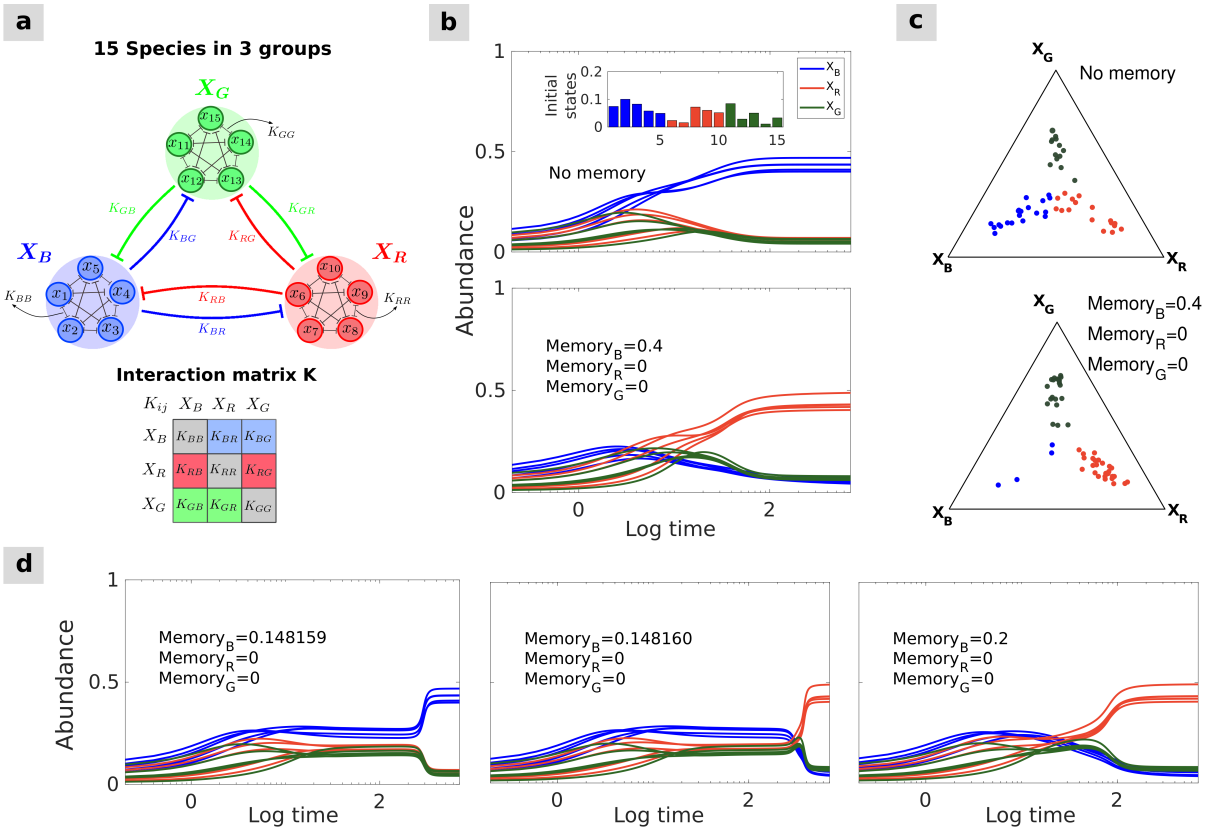

Fig 5. Impact of incommensurate memory on the community stability landscape: regime shifts without perturbation. (a) A simulated mutual interaction model with 15 species in three groups, blue, red, and green (see [18]). The interactions between species from different groups and within each group are illustrated. The within-group interactions are stronger than between-group interactions. **(b)** Starting from random initial conditions, the blue group of species dominates the community at the stable state when no memory is present (top). Imposing memory on the blue species leads to a temporary rise in abundance, but ultimately another (red) group of species dominates instead (bottom). **(c)** The stable state distributions of 50 simulations are represented by ternary plots. Each dot shows, for one simulation, the identity of the dominant group (color) and the average relative abundances of the three groups (position in the triangle) at convergence time (see Appendix S2 for details). In the memoryless system (top), the three groups roughly have the same chance of dominating the stable state, whereas imposing memory effects on the blue set of species (bottom) favors stable states where those species are not dominant. **(d)** Exceeding a particular threshold on incommensurate memory on the blue species (here, 0.14816) leads to an abrupt regime shift after a long period of subtle, gradual inclines, without changing any model parameters or adding noise.

Discussion

Our understanding of ecological community dynamics heavily relies on mathematical modeling. Dynamical community modeling is a particularly active research area in microbial ecology, where recent studies have proposed numerous mechanistic models of microbial community dynamics exploring the role of interactions, stochasticity, and external factors [1, 18, 42–44]. These studies have, however, largely neglected the role of ecological memory despite its potentially remarkable impact on community variation.

We have shown how ecological memory can be incorporated into models of microbial community

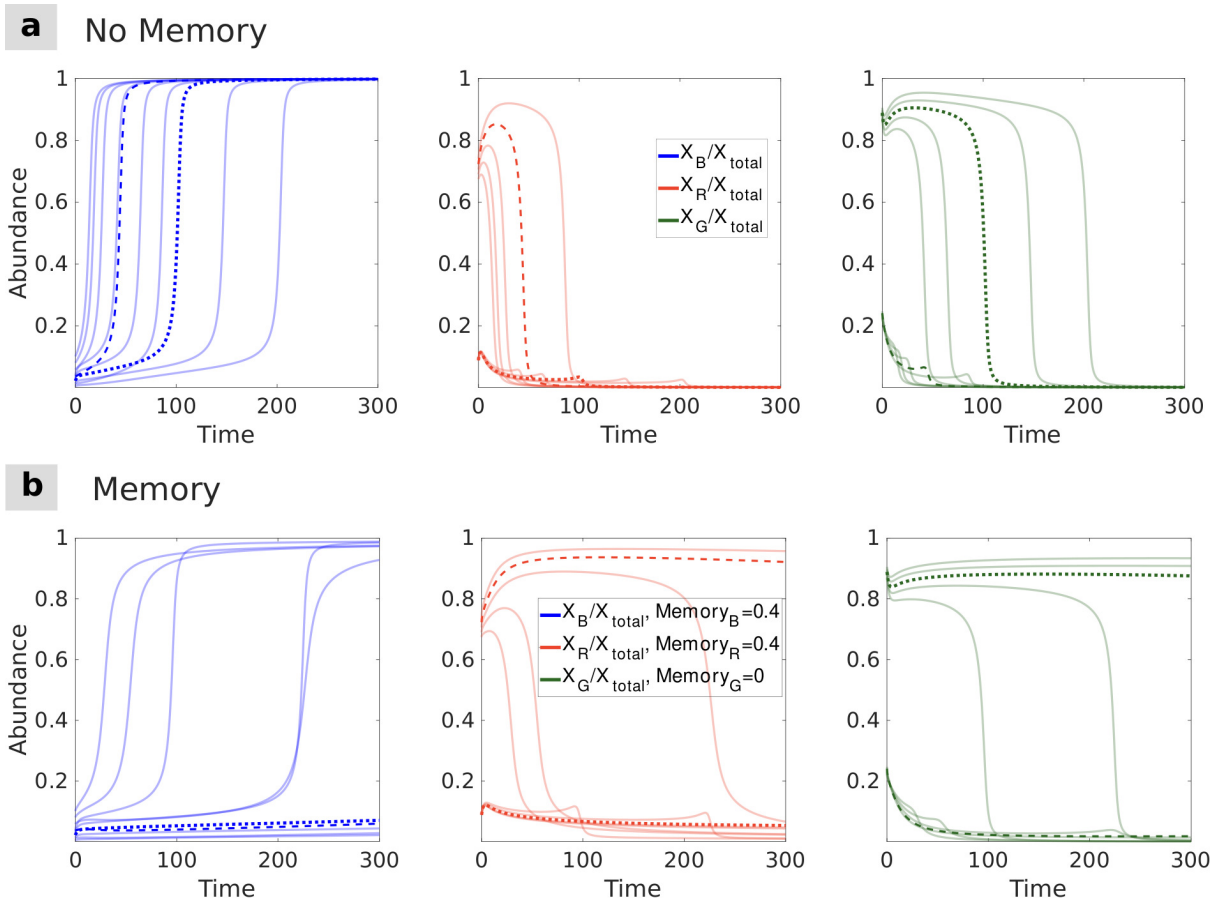

Fig 6. Incommensurate memory can induce multistability. Three-species community model that converges: **(a)** in the absence of memory, to a single stable state irrespective of initial abundances (see Fig S3), and **(b)** in the presence of incommensurate memory, to different stable states depending on species initial abundances. In each row, the three panels show the relative abundances of the blue, red and green species along time for the same set of initial conditions. In (b), the dashed and doted lines indicate the initial abundance thresholds that separate the three alternative attractor states, each corresponding to the dominance of a different species. No change in stable state is observed for the same values in the corresponding memoryless system (a).

dynamics, and used this modeling tool to demonstrate the role of memory as a potential key determinant of community dynamics. This has allowed us to expand our understanding of the impact of memory on community response to perturbation, long transient dynamics, delayed regime shifts, and the emergence of alternative community states.

Ecological communities are constantly subject to perturbations arising from external factors, as well as from internal processes and interactions between community members. Environmental fluctuations through time have a fundamental influence on ecological communities: they may promote species coexistence, increase community diversity [45,46], contribute to the properties of stable states [37,47], and in some cases, facilitate abrupt regime shifts [47]. Our analysis of memory in perturbed communities is closely linked to recent studies analysing the response of experimental microbial communities to antibiotic pulse perturbation [48, 49], or the impact of periodic perturbations on the evolution of antimicrobial

resistance [34].

Our approach is based on fractional calculus [32], a well-known mathematical framework with a broad range of applications [50, 51]. In this framework, ecological memory is represented by fractional derivatives and their associated kernel, which determines how quickly the influence of past states fades out (see Appendix S1). Commensurate fractional derivatives have previously been shown to cause intrinsic damping in a system [52–54], which may delay transitions or shift critical thresholds [33]. Incommensurate models, on the other hand, yield complicated ODE systems that are mathematically more challenging to analyse and therefore remain less well understood. We have shown here that the type of memory introduced by fractional derivatives can influence resistance and resilience in ecological communities. Quantifying this influence using recently proposed resilience measures, such as exit time [55], would provide a promising line of research for future work. While this framework allows introducing only a specific type of memory, our qualitative results on the influence of memory on community dynamics are likely to hold more generally.

In addition to damping, memory can also induce other dynamical properties, such as long periods of instability [36], or long transients [38], which have been reported in ecological systems [56] and chemostat experiments [57]. Long transients have previously been shown to be favored by stochasticity, multiple time scales, and high dimensionality [38], and our results indicate that memory should be added to this list; [38] also argue that regime shifts may occur during such long transient dynamics, without requiring parameter changes. Our results support this view, since we have shown that changes in incommensurate memory can trigger abrupt regime shifts even in the absence of perturbations.

Modeling real systems using models that incorporate memory would benefit from the ability to gather empirical evidence for the presence, strength, and quality of memory in the system. Recent literature suggests that it might indeed be possible to empirically detect the presence of memory based on the broad properties of a time series. It has been shown that longitudinal time series of microbial communities may carry detectable signatures of underlying ecological processes [4, 58]; and recently, Bayesian hierarchical models [10, 14], Random Forests [11], neural networks [59], and unsupervised Hebbian learning [60] have been proposed to detect signatures of memory in other contexts.

Several extensions of our model could be considered in future studies to enhance its flexibility and model memory more generally, such as varying initial times [33] or applying fractional differential equations with time-varying derivative orders [61]. Alternative approaches have also been considered to model ecological memory. These include the incorporation of autocorrelation or fixed time-lags into the model structure [15]. One could also model ecological memory by distributed delay differential equations (DDE) [62], fractional delay differential equations [63], or an integer memory-dependent derivative [64] with arbitrary kernel functions to shape different patterns of memory weights.

Ecological memory is a systemic property that can arise through various mechanisms. For instance, communities can alter their environment and thus modify environmental parameters in ways that reflect past events, or organisms may exhibit context-specific growth patterns that reflect adaptations [60, 65, 66]. Delay effects could also arise without memory and through other mechanisms, such as intracellular inertia. Species may indeed have different and often variable lag phases, due to complex intracellular processes that may be effectively memoryless. In such cases, the dampening effects could be simply modeled by introducing a "*break*" that would slow down or create a lag in community dynamics without inducing actual memory effects. Specifically designed longitudinal experiments could help evaluate the types and relative strengths of memory in real communities, such as in synthethic microbial communities that can be used to collect long and dense time series with highly controlled perturbations and replicated experiments.

Improving our understanding of the key mechanisms underlying community dynamics is a necessity to generate more accurate predictions, and ultimately to develop new techniques for the manipulation of complex ecological communities. We have combined theoretical analysis with computational simulations to explore the various facets of the influence of ecological memory and highlighted its often overlooked role as a key determinant of complex community dynamics.

References

1. Gonze D, Coyte KZ, Lahti L, Faust K. Microbial communities as dynamical systems. Curr Opin Microbiol. 2018;44:41–49. doi:10.1016/j.mib.2018.07.004.

2. Quince C, Walker AW, Simpson JT, Loman NJ, Segata N. Shotgun metagenomics, from sampling to analysis. Nat biotechnol. 2017;35(9):833–844. doi:10.1038/nbt.3935.

3. Song HS, Cannon WR, Beliaev AS, Konopka A. Mathematical Modeling of Microbial Community Dynamics: A Methodological Review. Processes. 2014;2(4):711–752. doi:10.3390/pr2040711.

4. Faust K, Bauchinger F, Laroche B, De Buyl S, Lahti L, Washburne AD, et al. Signatures of ecological processes in microbial community time series. Microbiome. 2018;6(1):1–13. doi:10.1186/s40168-018-0496-2.

5. Coenen AR, Hu SK, Luo E, Muratore D, Weitz JS. A Primer for Microbiome Time-Series Analysis. Front genet. 2020;11:310–310. doi:10.3389/fgene.2020.00310.

6. Björk JR, Dasari M, Grieneisen L, Archie EA. Primate microbiomes over time: Longitudinal answers to standing questions in microbiome research. American Journal of Primatology. 2019;81(10-11):e22970. doi:10.1002/ajp.22970.

7. Fukuyama J, Rumker L, Sankaran K, Jeganathan P, Dethlefsen L, Relman DA, et al. Multidomain analyses of a longitudinal human microbiome intestinal cleanout perturbation experiment. PLoS Comput Biol. 2017;13(8):1–29. doi:10.1371/journal.pcbi.1005706.

8. Gunderson LH. Ecological Resilience—in Theory and Application. Annu Rev Ecol Evol Syst. 2000;31(1):425–439. doi:10.1146/annurev.ecolsys.31.1.425.

9. Johnstone JF, Allen CD, Franklin JF, Frelich LE, Harvey BJ, Higuera PE, et al. Changing disturbance regimes, ecological memory, and forest resilience. Front Ecol Environ. 2016;14(7):369–378. doi:10.1002/fee.1311.

10. Ogle K, Barber JJ, Barron-Gafford GA, Bentley LP, Young JM, Huxman TE, et al. Quantifying ecological memory in plant and ecosystem processes. Ecol Lett. 2015;18(3):221–235. doi:10.1111/ele.12399.

11. Benito BM, Gil-Romera G, Birks HJB. Ecological memory at millennial time-scales: the importance of data constraints, species longevity and niche features. Ecography. 2020;43(1):1–10. doi:10.1111/ecog.04772.

12. Schweiger AH, Boulangeat I, Conradi T, Davis M, Svenning JC. The importance of ecological memory for trophic rewilding as an ecosystem restoration approach. Biol Rev. 2019;94(1):1–15. doi:10.1111/brv.12432.

13. Žliobaitė I, Fortelius M, Stenseth NC. Reconciling taxon senescence with the Red Queen's hypothesis. Nature. 2017;552(7683):92–95. doi:10.1038/nature24656.

14. Itter MS, Vanhatalo J, Finley AO. EcoMem: An R package for quantifying ecological memory. Environ Model Softw. 2019;119:305–308. doi:10.1016/j.envsoft.2019.06.004.

15. Golinski M, Bauch C, Anand M. The effects of endogenous ecological memory on population stability and resilience in a variable environment. Ecol Model. 2008;212(3):334–341. doi:10.1016/j.ecolmodel.2007.11.005.

16. Schaefer V. Alien invasions, ecological restoration in cities and the loss of ecological memory. Restor Ecol. 2009;17(2):171–176. doi:10.1111/j.1526-100X.2008.00513.x.

17. Bengtsson J, Angelstam P, Elmqvist T, Emanuelsson U, Folke C, Ihse M, et al. Reserves, resilience and dynamic landscapes. Ambio. 2003;32(6):389–396. doi:10.1579/0044-7447-32.6.389.

18. Gonze D, Lahti L, Raes J, Faust K. Multi-stability and the origin of microbial community types. ISME J. 2017;11(10):2159. doi:10.1038/ismej.2017.60.

19. Gibson T, Gerber G. Robust and Scalable Models of Microbiome Dynamics. In: Proceedings of the 35th International Conference on Machine Learning. vol. 80. PMLR; 2018. p. 1763–1772.

20. Marino S, Baxter NT, Huffnagle GB, Petrosino JF, Schloss PD. Mathematical modeling of primary succession of murine intestinal microbiota. Proc Natl Acad Sci USA. 2014;111(1):439–444.

21. Stein RR, Bucci V, Toussaint NC, Buffie CG, Rätsch G, Pamer EG, et al. Ecological modeling from time-series inference: insight into dynamics and stability of intestinal microbiota. PLoS Comput Biol. 2013;9(12):e1003388. doi:10.1371/journal.pcbi.1003388.

22. Bucci V, Tzen B, Li N, Simmons M, Tanoue T, Bogart E, et al. MDSINE: Microbial Dynamical Systems INference Engine for microbiome time-series analyses. Genome Biol. 2016;17(1):1–17. doi:10.1186/s13059-016-0980-6.

23. Shenhav L, Furman O, Briscoe L, Thompson M, Silverman JD, Mizrahi I, et al. Modeling the temporal dynamics of the gut microbial community in adults and infants. PLoS Comput Biol. 2019;15(6):e1006960. doi:10.1371/journal.pcbi.1006960.

24. Li C, Chng KR, Kwah JS, Av-Shalom TV, Tucker-Kellogg L, Nagarajan N. An expectation-maximization algorithm enables accurate ecological modeling using longitudinal microbiome sequencing data. Microbiome. 2019;7(1):1–14. doi:10.1186/s40168-019-0729-z.

25. Joseph TA, Shenhav L, Xavier JB, Halperin E, Pe'er I. Compositional Lotka-Volterra describes microbial dynamics in the simplex. PLoS Comput Biol. 2020;16(5):e1007917. doi:10.1371/journal.pcbi.1007917.

26. McGeachie MJ, Sordillo JE, Gibson T, Weinstock GM, Liu YY, Gold DR, et al. Longitudinal prediction of the infant gut microbiome with dynamic bayesian networks. Sci Rep. 2016;6:20359. doi:10.1038/srep20359.

27. Ravel J, Gajer P, Abdo Z, Schneider GM, Koenig SSK, McCulle SL, et al. Vaginal microbiome of reproductive-age women. Proc Natl Acad Sci USA. 2011;108(Supplement 1):4680–4687. doi:10.1073/pnas.1002611107.

28. Falony G, Joossens M, Vieira-Silva S, Wang J, Darzi Y, Faust K, et al. Population-level analysis of gut microbiome variation. Science. 2016;352(6285):560–564. doi:10.1126/science.aad3503.

29. Arumugam M, Raes J, Pelletier E, Le Paslier D, Yamada T, Mende DR, et al. Enterotypes of the human gut microbiome. Nature. 2011;473(7346):174–180. doi:10.1038/nature09944.

30. Ding T, Schloss PD. Dynamics and associations of microbial community types across the human body. Nature. 2014;509(7500):357–360. doi:10.1038/nature13178.

31. Costea PI, Hildebrand F, Arumugam M, Bäckhed F, Blaser MJ, Bushman FD, et al. Enterotypes in the landscape of gut microbial community composition. Nat Microbiol. 2018;3(1):8–16. doi:10.1038/s41564-017-0072-8.

32. Du M, Wang Z, Hu H. Measuring memory with the order of fractional derivative. Sci Rep. 2013;3(1):1–3. doi:10.1038/srep03431.

33. Saeedian M, Khalighi M, Azimi-Tafreshi N, Jafari GR, Ausloos M. Memory effects on epidemic evolution: The susceptible-infected-recovered epidemic model. Phys Rev E. 2017;95:022409. doi:10.1103/PhysRevE.95.022409.

34. Marrec L, Bitbol AF. Resist or perish: Fate of a microbial population subjected to a periodic presence of antimicrobial. PLoS Comput Biol. 2020;16(4):e1007798. doi:10.1371/journal.pcbi.1007798.

35. Rivero M, Rogosin SV, Tenreiro Machado JA, Trujillo JJ. Stability of fractional order systems. Math Probl Eng. 2013;2013:356215. doi:10.1155/2013/356215.

36. Spanbauer TL, Allen CR, Angeler DG, Eason T, Fritz SC, Garmestani AS, et al. Prolonged instability prior to a regime shift. PLoS One. 2014;9(10). doi:10.1371/journal.pone.0108936.

37. Tropini C, Moss EL, Merrill BD, Ng KM, Higginbottom SK, Casavant EP, et al. Transient osmotic perturbation causes long-term alteration to the gut microbiota. Cell. 2018;173(7):1742–1754. doi:10.1016/j.cell.2018.05.008.

38. Hastings A, Abbott KC, Cuddington K, Francis T, Gellner G, Lai YC, et al. Transient phenomena in ecology. Science. 2018;361(6406):eaat6412. doi:10.1126/science.aat6412.

39. Amirian MM, Towers IN, Jovanoski Z, Irwin AJ. Memory and mutualism in species sustainability: A time-fractional Lotka-Volterra model with harvesting. Heliyon. 2020;6(9):e04816. doi:10.1016/j.heliyon.2020.e04816.

40. Khalighi M, Eftekhari L, Hosseinpour S, Lahti L. Three-species Lotka-Volterra model with respect to Caputo and Caputo-Fabrizio fractional operators. Symmetry. 2021;13(3):368. doi:10.3390/sym13030368.

41. Sommer F, Anderson JM, Bharti R, Raes J, Rosenstiel P. The resilience of the intestinal microbiota influences health and disease. Nat Rev Microbiol. 2017;15(10):630–638. doi:10.1038/nrmicro.2017.58.

42. Khazaei T, Williams RL, Bogatyrev SR, Doyle JC, Henry CS, Ismagilov RF. Metabolic multistability and hysteresis in a model aerobe-anaerobe microbiome community. Sci Adv. 2020;6(33):eaba0353. doi:10.1126/sciadv.aba0353.

43. Bush T, Diao M, Allen RJ, Sinnige R, Muyzer G, Huisman J. Oxic-anoxic regime shifts mediated by feedbacks between biogeochemical processes and microbial community dynamics. Nat Commun. 2017;8(1):1–9. doi:https://doi.org/10.1038/s41467-017-00912-x.

44. Goyal A, Dubinkina V, Maslov S. Multiple stable states in microbial communities explained by the stable marriage problem. ISME J. 2018;12(12):2823–2834. doi:10.1038/s41396-018-0222-x.

45. Hutchinson GE. The paradox of the plankton. Am Nat. 1961;95(882):137–145. doi:10.1086/282171.

46. Huston M. A general hypothesis of species diversity. Am Nat. 1979;113(1):81–101. doi:10.1086/283366.

47. Abreu CI, Andersen Woltz VL, Friedman J, Gore J. Microbial communities display alternative stable states in a fluctuating environment. PLoS Comput Biol. 2020;16(5):1–17. doi:10.1371/journal.pcbi.1007934.

48. Cairns J, Jokela R, Becks L, Mustonen V, Hiltunen T. Repeatable ecological dynamics govern the response of experimental communities to antibiotic pulse perturbation. Nat Ecol Evol. 2020;4(10):1385–1394. doi:10.1038/s41559-020-1272-9.

49. Hiltunen T, Virta M, Laine AL. Antibiotic resistance in the wild: an eco-evolutionary perspective. Philos Trans R Soc Lond, B, Biol Sci. 2017;372(1712):20160039. doi:10.1098/rstb.2016.0039.

50. Sun H, Zhang Y, Baleanu D, Chen W, Chen Y. A new collection of real world applications of fractional calculus in science and engineering. Commun Nonlinear Sci Numer Simul. 2018;64:213–231. doi:10.1016/j.cnsns.2018.04.019.

51. Almeida R, Bastos NR, Monteiro MTT. Modeling some real phenomena by fractional differential equations. Math Methods Appl Sci. 2016;39(16):4846–4855. doi:10.1002/mma.3818.

52. Achar BNN, Hanneken JW, Clarke T. Response characteristics of a fractional oscillator. Physica A. 2002;309(3):275–288. doi:10.1016/S0378-4371(02)00609-X.

53. Tarasov VE. Quantum dissipation from power-law memory. Ann Phys (N Y). 2012;327(6):1719–1729. doi:10.1016/j.aop.2012.02.011.

54. Tofighi A. The intrinsic damping of the fractional oscillator. Physica A. 2003;329(1):29–34. doi:10.1016/S0378-4371(03)00598-3.

55. Arani BMS, Carpenter SR, Lahti L, van Nes EH, Scheffer M. Exit time as a measure of ecological resilience. Science. 2021;372(6547). doi:10.1126/science.aay4895.

56. Morozov A, Abbott K, Cuddington K, Francis T, Gellner G, Hastings A, et al. Long transients in ecology: Theory and applications. Phys Life Rev. 2020;32:1–40. doi:10.1016/j.plrev.2019.09.004.

57. Fukami T. Assembly history interacts with ecosystem size to influence species diversity. Ecology. 2004;85(12):3234–3242. doi:10.1890/04-0340.

58. Faust K, Lahti L, Gonze D, de Vos WM, Raes J. Metagenomics meets time series analysis: unraveling microbial community dynamics. Curr Opin Microbiol. 2015;25:56–66. doi:10.1016/j.mib.2015.04.004.

59. Armstrong McKay DI, Dyke JG, Doncaster CP, Dearing JA, Wang R. Network-based metrics of resilience and ecological memory in lake ecosystems. bioRxiv. 2020;doi:10.1101/810762.

60. Power DA, Watson RA, Szathmáry E, Mills R, Powers ST, Doncaster CP, et al. What can ecosystems learn? Expanding evolutionary ecology with learning theory. Biology Direct. 2015;10(1):69. doi:10.1186/s13062-015-0094-1.

61. Sun H, Chang A, Zhang Y, Chen W. A review on variable-order fractional differential equations: mathematical foundations, physical models, numerical methods and applications. Fract Calc Appl Anal. 2019;22(1):27–59. doi:10.1142/S0218127412300145.

62. Cooke KL, Grossman Z. Discrete delay, distributed delay and stability switches. J Math Anal Appl. 1982;86(2):592–627. doi:10.1016/0022-247X(82)90243-8.

63. Zúñiga-Aguilar C, Coronel-Escamilla A, Gómez-Aguilar J, Alvarado-Martínez V, Romero-Ugalde H. New numerical approximation for solving fractional delay differential equations of variable order using artificial neural networks. Eur Phys J Plus. 2018;133(2):1–16. doi:10.1140/epjp/i2018-11917-0.

64. Wang JL, Li HF. Memory-dependent derivative versus fractional derivative (I): Difference in temporal modeling. J Comput Appl Math. 2021;384:112923. doi:10.1016/j.cam.2020.112923.

65. Miller AD, Inamine H, Buckling A, Roxburgh SH, Shea K. How disturbance history alters invasion success: biotic legacies and regime change. Ecol Lett. 2021;24(4):687–697. doi:10.1111/ele.13685.

66. Yen P, Papin JA. History of antibiotic adaptation influences microbial evolutionary dynamics during subsequent treatment. PLoS Biol. 2017;15(8):1–34. doi:10.1371/journal.pbio.2001586.

67. Safdari H, Kamali MZ, Shirazi A, Khalighi M, Jafari G, Ausloos M. Fractional dynamics of network growth constrained by aging node interactions. PLoS One. 2016;11(5):e0154983. doi:10.1371/journal.pone.0154983.

68. Li C, Zhang F. A survey on the stability of fractional differential equations. Eur Phys J Spec Top. 2011;193(1):27–47. doi:10.1140/epjst/e2011-01379-1.

69. Emir K. Stability analysis of fractional differential equations with unknown parameters. Nonlinear Anal Model Control. 2019;24(2):224–240. doi:10.15388/NA.2019.2.5.

70. Petráš I. Chaos in fractional-order population model. Int J Bifurc Chaos Appl Sci Eng. 2012;22(04):1250072. doi:10.1142/S0218127412500721.

71. de Oliveira EC, Tenreiro Machado JA. A Review of Definitions for Fractional Derivatives and Integral. Math Probl Eng. 2014;2014. doi:10.1155/2014/238459.

72. Caputo M. Linear models of dissipation whose Q is almost frequency independent–II. Geophys J Int. 1967;13(5):529–539. doi:10.1111/j.1365-246X.1967.tb02303.x.

73. Kilbas AA, Srivastava HM, Trujillo JJ. Theory and applications of fractional differential equations. vol. 204. Elsevier; 2006.

74. Podlubny I. Fractional differential equations: An introduction to fractional derivatives, fractional differential equations, to methods of their solution and some of their applications. Elsevier; 1998.

75. Diethelm K, Ford NJ, Freed AD. A predictor-corrector approach for the numerical solution of fractional differential equations. Nonlinear Dyn. 2002;29(1-4):3–22. doi:10.1023/A:1016592219341.

76. Garrappa R. On linear stability of predictor–corrector algorithms for fractional differential equations. Int J Comput Math. 2010;87(10):2281–2290. doi:10.1080/00207160802624331.

77. Khalighi M. moeinkh88/Moein-Khalighi: article_2021_memoryeffects; 2021. Zenodo. Available from: `https://doi.org/10.5281/zenodo.4725218`.

78. Diethelm K, Ford NJ, Freed AD. Detailed error analysis for a fractional Adams method. Numer Algorithms. 2004;36(1):31–52. doi:10.1023/B:NUMA.0000027736.85078.be.

Supporting information

Appendix S1

In the following, we detail the mathematical aspects of incorporating ecological memory into a non-linear extension of the generalized Lotka-Volterra model.

Memoryless model

We used as a starting point the following memoryless model, introduced by [18]:

$$\begin{aligned} \frac{dX_i}{dt} &= X_i \left(b_i f_i(\{X_k\}) - k_i X_i \right), \\ f_i(\{X_k\}) &= \prod_{\substack{k=1 \\ k \neq i}}^{N} \frac{K_{ik}^n}{K_{ik}^n + X_k^n}. \end{aligned} \tag{1}$$

This model describes the dynamics of each microbial species abundance X_i according to its growth rate b_i, its death rate k_i and an inhibition term f_i, which is defined by interaction constants K_{ij} and the Hill coefficient n as parameters. K_{ij} represents the inhibition of species i by species j: the lower it is, the stronger the inhibition.

The interaction matrix $\mathbf{K} = \{K_{ij}\}$ was generated based on two alternative approaches. The first approach allocates the predefined species in three groups (see below and Fig 5 as in [18]), thereby setting different values of inter-group versus intra-group interactions. The second approach does not impose a predefined structure for the interaction matrix $\mathbf{K}$ (Fig S4).

Three-group model

In the three-group approach, we define three sets of species indices by B (blue), R (red), and G (green). Each species i belongs to exactly one of these three groups. We define the growth rate of each group by the growth vector $\mathbf{b} = [b_B,\ b_R,\ b_G]$, where $b_B = \{b_i \mid i \in B\}$, $b_R = \{b_i \mid i \in R\}$, and $b_G = \{b_i \mid i \in G\}$. We also define the interaction matrix $\mathbf{K} = \{K_{ij} \mid i, j \in B\ or\ R\ or\ G\}$ such that K_{ij} only depends on the group memberships of species i and j, up to a slight noise (see Fig 5a and Appendix S2). We first considered a community of three species (*i.e.*, only one species per group), and then a community of 15 species forming three groups with strong inter-group inhibition and weak intra-group inhibition.

If the inhibition strength is large enough (small K_{ij}), this model can have three coexisting stable states (tristability). This tristable community is dominated by either one of its three groups depending on initial species abundances, interaction matrix $\mathbf{K}$, and growth vector $\mathbf{b}$.

Incorporating memory by fractional calculus

Fractional order derivatives have been successfully used to account for memory effects in many disciplines [32, 33, 67]. This approach requires defining a temporal kernel in dynamical models [32, 33]. The stable regions of fractional differential equations differ from the corresponding classical one [35, 68, 69] and thus induce significant differences in the stability landscape of a community model. Interestingly, *chaos* has been observed in a fractional population model [70], which exhibits a structure entirely different from typical dynamical attractors such as the Rössler or Lorenz attractors.

To introduce memory in ODE models, we replace the ordinary time derivative in system (1) by the fractional derivative $\mathfrak{D}^{\mu_i}$. This leads to the appearance of a time correlation function (a memory kernel) which imposes a dependency between the current system state and its past trajectory. The past states of the system influence the current dynamics, giving rise to memory effects.

Let us now rewrite the initial model in (1) by employing fractional derivatives and the simplifying notation $F_i = F(t, X_i) := X_i \left(b_i f_i(\{X_k\}) - k_i X_i\right)$, as:

$$\mathfrak{D}^{\mu_i} X_i = F_i, \quad 0 < \mu_i \leq 1, \mu_i \in \mathbb{R}. \tag{2}$$

There are different definitions of fractional time derivatives for different purposes [71]. We use here the Caputo fractional time derivative [72], $\mathfrak{D}^{\mu_i} := {}_{t_0}^{c}D_t^{\mu_i}$, as a control parameter of memory effects because of its intuitive interpretation. This derivative is defined by the following integral equation for a given function $g(t)$:

$${}_{t_0}^{c}D_t^{\mu} g(t) = {}_{t_0}I_t^{1-\mu} g'(t) = \frac{1}{\Gamma(1-\mu)} \int_{t_0}^{t} \frac{g'(\tau) d\tau}{(t-\tau)^{\mu}}, \quad 0 < \mu \leq 1, \tag{3}$$

in which ${}_{t_0}I_t^{1-\mu}$ is the fractional integral of order $1-\mu$ that is defined by

$${}_{t_0}I_t^{\mu} g(t) = \frac{1}{\Gamma(\mu)} \int_{t_0}^{t} \frac{g(\tau) d\tau}{(t-\tau)^{1-\mu}}, \tag{4}$$

where Γ denotes the gamma function. Throughout this article, we quantify memory as $1-\mu$.

Model interpretation

To provide an intuitive interpretation of the new system equation (2), let us apply a fractional Caputo derivative of order $1-\mu_i$ on both sides of (2):

$${}_{t_0}^{c}D_t^{1-\mu_i} \left({}_{t_0}^{c}D_t^{\mu_i} X_i \right) = {}_{t_0}^{c}D_t^{1-\mu_i} \left(F_i \right). \tag{5}$$

Because the Caputo fractional derivatives of order μ and $-\mu$ are inverse operators [73, 74], this simplifies as:

$$ {}_{t_0}^{c}D_t^1 X_i = \frac{dX_i}{dt} = {}_{t_0}^{c}D_t^{1-\mu_i}\left(F_i\right). \tag{6} $$

Equation (6) shows that for $\mu_i = 1$ we retrieve the standard integer derivative model (1) as a special case of the fractional derivative model (2), since the fractional operator becomes the unity operator for a fractional order of 1. Furthermore, the right-hand side of equation (6) can be expressed as the fractional integral of order $(\mu_i - 1)$ on the interval $[t_0, t]$, that is:

$$ \frac{dX_i(t)}{dt} = \frac{1}{\Gamma(\mu_i - 1)} \int_{t_0}^{t} (t-\tau)^{\mu_i - 2} F(\tau, X_i) d\tau. \tag{7} $$

The system described by equation (7) is a transformation of the original system (1) with an additional memory contributions μ_i. When $0 < \mu_i < 1$, the time-dependent memory kernel $\frac{1}{\Gamma(\mu_i-1)}(t-\tau)^{\mu_i-2}$ guarantees the existence of temporal scaling behaviors which are common in nature. The memory kernel's decay rate depends on μ_i: the lower the value of μ_i, the slower it will decay. This shows how imposing memory on the system equation (1) slows down community dynamics.

The derivative order μ_i can be used to control the strength of the memory so that when μ_i goes toward the integer value 1, the influence of memory decreases, and the system tends toward a Markov process. In the context of microbial communities, memory may thus counteract the effects of species interactions. In the memoryless case ($\mu_i = 1$), the kernel becomes a Dirac delta function, $\delta(t-\tau)$, which results in the integer-order integrodifferential equation of model (1).

In summary, the Caputo fractional derivative provide a means to incorporate ecological memory in a dynamical system based on a convolution integral with a power-law memory kernel. Besides, it could be modified by a time-delay reflecting the duration of memory effects and the kernel function shaping the memory weight [64].

Numerical simulations

Adams methods provide commonly used numerical solutions for ODEs, involving implicit (Adams-Moulton) and explicit (Adams-Bashforth) linear multi-step schemes. We exploited in this paper the predictor-corrector method based on Adams formulae (see [75, 76]) and implemented it in MATLAB. The corresponding code is available on Zenodo [77].

Given the system equation (2), let us write $\mathbf{X}$ the set of all species abundances, $\boldsymbol{\mu}$ the corresponding vector of derivative orders μ_i, and $\mathbf{F}$ the corresponding matrix function of all $X_i\left(b_i f_i(\{X_k\}) - k_i X_i\right)$. We can then rewrite the fractional order model (2) in the following matrix form:

$$ \mathfrak{D}^{\boldsymbol{\mu}}\mathbf{X} = \mathbf{F}(t, \mathbf{X}), \text{ where } \mathbf{X}(t_0) = \mathbf{X}_0. \tag{8} $$

The initial value problem (8) is equivalent to the Volterra integral equation [73, 75]:

$$\mathbf{X}(t) = \mathbf{X}_0 + \frac{1}{\Gamma(\boldsymbol{\mu})} \int_{t_0}^{t} (t-\tau)^{\boldsymbol{\mu}-1} \mathbf{F}(\tau, \mathbf{X}(\tau)) d\tau. \tag{9}$$

We solved Eq. (9) using a product integration technique, in which we replaced the function $\mathbf{F}(\tau, \mathbf{X}(\tau))$ with piece-wise interpolating polynomials. For the grid nodes t_j $(j = 0, ..., m)$ with constant step size h $(t_j = t_0 + jh)$, we write $\mathbf{F}_j = \mathbf{F}(t_j, \mathbf{X}_j)$ where $\mathbf{X}_j$ is the numerical approximation to $\mathbf{X}(t_j)$. The product rectangle rule [75] gives an explicit estimation of Eq. (9) as a predictor:

$$\begin{aligned} \mathbf{X}_m &= \mathbf{X}_0 + h^{\boldsymbol{\mu}} \textstyle\sum_{j=0}^{m-1} \mathbf{b}_{m-j-1} \mathbf{F}_j, \\ \mathbf{b}_{m-j-1} &= \tfrac{(m-j)^{\boldsymbol{\mu}} - (m-j-1)^{\boldsymbol{\mu}}}{\Gamma(\boldsymbol{\mu}+1)}, \end{aligned} \tag{10}$$

and the product trapezoidal rule [75] provides an implicit estimation of Eq. (9) as a corrector:

$$\begin{aligned} \mathbf{X}_m &= \mathbf{X}_0 + h^{\boldsymbol{\mu}} \mathbf{c}_m \mathbf{F}_0 + h^{\boldsymbol{\mu}} \textstyle\sum_{j=1}^{m} \mathbf{d}_{m-j} \mathbf{F}_j, \\ \mathbf{c}_m &= \tfrac{(m-1)^{\boldsymbol{\mu}+1} - m^{\boldsymbol{\mu}}(m-\boldsymbol{\mu}-1)}{\Gamma(\boldsymbol{\mu}+2)}, \\ \mathbf{d}_{m-j} &= \begin{cases} \frac{1}{\Gamma(\boldsymbol{\mu}+2)}, & \text{if } m-j=0, \\ \frac{(m-j-1)^{\boldsymbol{\mu}+1} - 2(m-j)^{\boldsymbol{\mu}+1} + (m-j+1)^{\boldsymbol{\mu}+1}}{\Gamma(\boldsymbol{\mu}+2)}, & \text{if } m-j=1,2,... \end{cases} \end{aligned} \tag{11}$$

The last term of the sum in the corrector equation (11), $\mathbf{F}(t_m, \mathbf{X}_m)$, is obtained by an approximation of $\mathbf{X}_m$ in the predictor equation (10). This method is called FracPECE: Fractional Predict-Evaluate-Correct-Evaluate [75]. Because its standard implementation was not sufficient considering the stiffness of the equation, we improved its accuracy via an advanced convolution quadrature [76], and via multiple applications of the corrector step [78] when required. Specifically, we used several corrector iterations when the difference between two consecutive iterations was larger than the desired tolerance of 10^{-6}. We considered a time step size of $h = 0.01$ or 0.005 for all simulations.

Note that since the model with fractional order derivatives (2) includes the standard model (1) as a particular case (namely, for integer derivative order), the numerical approximations (10) and (11) are also solutions to equation (1). The explicit solution (10)–or an assessment of the implicit solution (11)–shows how memory influences the fundamental system dynamics through the dependence on μ.

Appendix S2

We provide in the Table below the detailed conditions and parameter values used in each of the numerical experiments presented in the main text. Additional methodological clarifications for figures 5c and S1 are given in the text below the table.

Table . Exact model specifications for the 3-species and 15-species systems.

Figure	X_0			K_{ij}	n	k_i	μ			b		
	B	R	G	$\forall i \neq j$		$\forall i$	B=R=G			B	R	G
2a	0.99	0.01	0.01	0.1	2	1	1 & 0.9			Pulse1	0.95	Pulse1
2b							1 & 0.9			Pulse2		Pulse2
3a							1 & 0.9 & 0.85			Pulse3		1.05
3b							1 & 0.96 & 0.9			Periodic		1.05
4b-c	1/3	1/3	1/3	0.1	2	1	1 0.9157959 0.9157954 0.9157952 0.9 0.7 0.6			Stochastic		
							B	R	G			
S1	Equilibrium points			Random interactions	4	2	No Specified Groups $\mu_{i,\ \forall i} = 1$ (or 0.7)			$\mathcal{N}(1, 0.0025)$ with a pulse		
S2a	0.99	0.01	0.01	0.1	2	1	1 1 1	1 1 1	1 0.90895 0.90893	Pulse4	0.95	1.05
S2b	1/3	1/3	1/3	0.1	2	1	1 1 1	1 1 0.9	1 0.8 1	Stochastic		
5	$Uniform(0, 0.1)$			Predefined interactions	2	1	1 0.6 0.851841 0.851840 0.8	1	1	$\mathcal{N}(1, 0.01)$		
S3 & **6a** **6b**	[0.005,0.05]	0.1&0.3	1&0.1	0.1	2	1	1 0.6	1 0.6	1 1	4	0.95	1.05
S4	0.25	0.25	0.25	0.2	2	0.5	1 1 0.5	1 0.4 0.6	1 0.7 1	$\mathcal{N}(1, 0.01)$		

Pulse1: $b_B(t) = 0.5$ and $b_G(t) = 2$ if $20 \leq t < 60$, otherwise $b_B(t) = 1$ and $b_G(t) = 1.05$.
Pulse2: $b_B(t) = 0.5$ and $b_G(t) = 2.2$ if $20 \leq t < 60$, otherwise $b_B(t) = 1$ and $b_G(t) = 1.05$.
Pulse3: $b_B(t) = 0.2$ if $60 \leq t < 100$, $b_B(t) = 4.5$ if $200 \leq t < 330$, otherwise $b_B(t) = 1$.
Periodic: $b_B(t) = 1$ if $20(2m-2) \leq t < 20(2m-1)$, $b_B(t) = 0.2$ if $20(4m-3) \leq t < 20(4m-2)$, $b_B(t) = 4.5$ if $20(4m-1) \leq t < 20(4m)$ where $m \in \mathbb{N}$.
Stochastic: The growth rates of these panels are generated by mean-reverting the Ornstein-Uhlenbeck Process described by the stochastic equation $db_t = \theta(\phi - b_t)dt + \sigma dW_t$.
Random interactions: $K_{ij} = 1 - e^{-5z}$, where z is randomly generated from a uniform distribution between 0 and 1.
Predefined interactions: $K_{ij} \sim 1 + \mathcal{N}(0, 0.01)$ for species i and j in the same group (intra-group interactions K_{BB}, K_{RR}, K_{GG}), and $K_{ij} \sim 0.5 + \mathcal{N}(0, 0.01)$ for species i and j in different groups (inter-group interactions).
Pulse4: $b_B(t) = 0.2$ if $60 \leq t < 100$, $b_B(t) = 4.5$ if $400 \leq t < 530$, otherwise $b_B(t) = 1$.

Fig 5c. Ternary plots allow representing the state of a 3-species or 3-group system by a single dot and therefore are a convenient way to display the outcome of many simulations at a time. In Fig 5c, each ternary plot shows the stable state distribution of the group relative abundances obtained for 50 different simulations, each represented by a dot of the color of the dominant group. We detail below how we computed the position of each dot in the triangle. Let us write B, G and R the average stable state

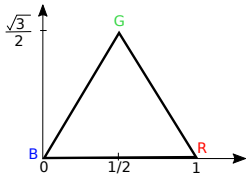

Fig . Triangle coordinates.

relative abundances of the species in the blue, green and red groups, that is $R = \frac{\sum_{i=1}^{5} R_i(end)}{\sum_i (R_i + B_i + G_i)(end)}$ (and similarly for B and G), where $Z_i(end)$ denotes the abundance of species i in group Z at the end of the simulation. Let us consider an equilateral triangle in which each vertex corresponds to the complete dominance of one group of species, as shown in the Figure above. Thus, a point (dot) close to the middle of the triangle indicates a state of the system characterized by relatively even species abundances. If $B = 1$ (100%) is placed at $(x, y) = (0, 0)$ and $R = 1$ (100%) at $(1, 0)$, then $G = 1$ (100%) is at $(\frac{1}{2}, \frac{\sqrt{3}}{2})$, and any triplet (B, R, G) will be at $[\frac{1}{2}(2R + G), \frac{\sqrt{3}}{2}G]$. These Cartesian coordinates provide a way to map any triplet of group relative abundances to a unique location on the triangle.

Fig S1. Here, we randomly generated an interaction matrix $\mathbf{K}$ without predefined structure between $N = 15$ species. Specifically, we set $n = 4$ and $K_{ij} = 1 - e^{-5z}$, where z is a randomly generated number from a uniform distribution between 0 and 1. We generated 10 communities, each with a random vector of growth rates generated as $b_i \sim \mathcal{N}(1, 0.0025)$, $\forall i$. We used the same interaction matrix for all 10 communities, and death rates $k_i = 2$, $\forall i$. For each community, we set the initial values for species abundances X_i at one of the equilibrium points of the system (randomly chosen). To compute the dissimilarity of the community between times t_r and t_p, we used the Bray-Curtis distance, computed as $BC(t_r, t_p) = \frac{\sum_{i=r}^{N} |X_i(t_r) - X_i(t_p)|}{\sum_{i=1}^{N} X_i(t_r) + X_i(t_p)}$.

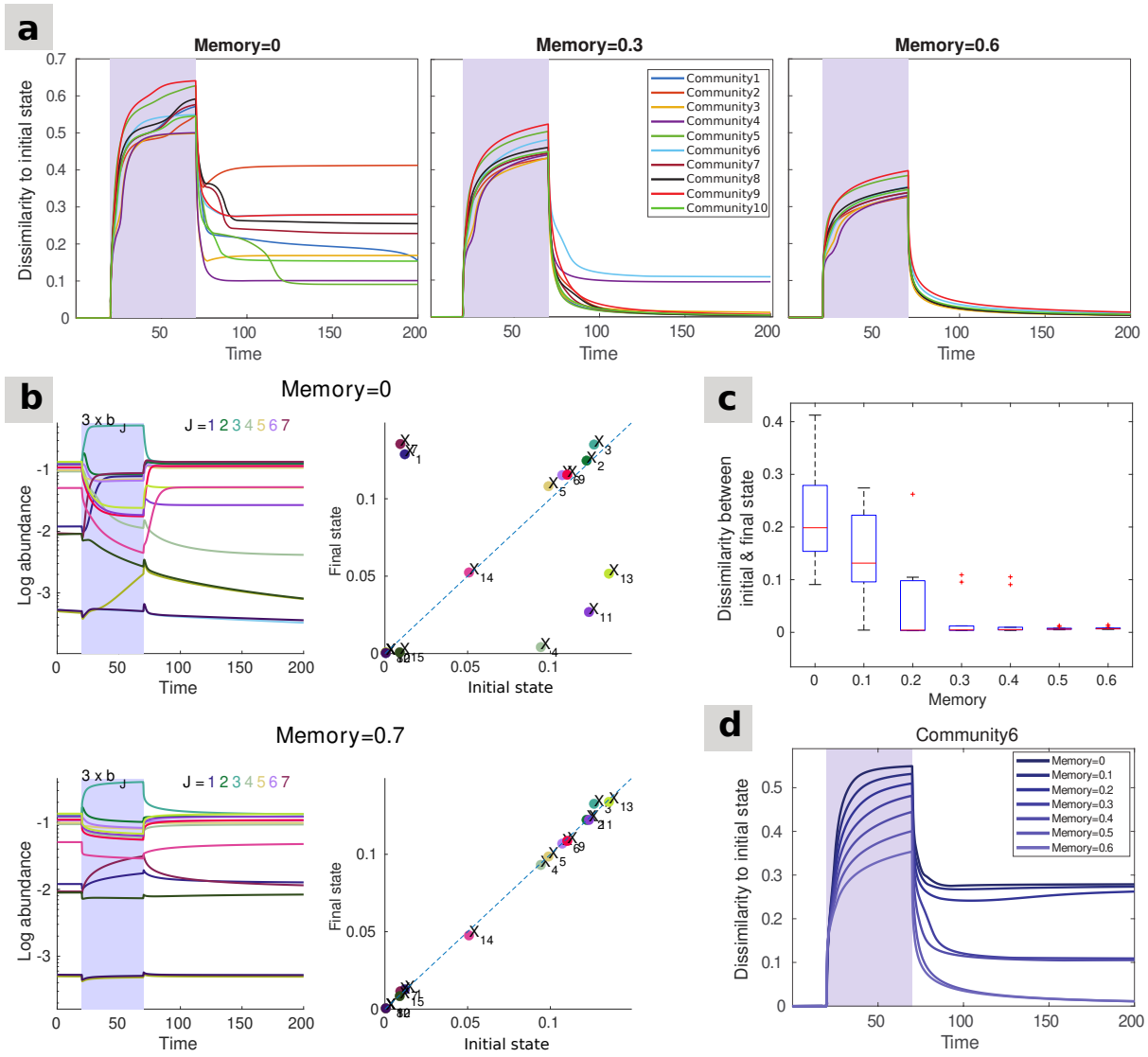

Fig S1. Memory effects preserve the stable state. We simulated ten communities of 15 species, each with random interaction matrices. A similar level of commensurate memory is applied to all ten communities. Every community is initially in a stable state of the system, and a perturbation is imposed by multiplying the growth rates of half of the species $(b_1, ..., b_7)$ by 3. The simulation is stopped when the system is close to its new stable state. Although only the effect of commensurate memory is illustrated here, the same outcome can be achieved using incommensurate memory. **(a)** Dissimilarity to the initial stable state through time for all ten communities, for three different memory strengths. The stronger the memory, the more constrained the community trajectories are, and the more likely they are to revert to their initial stable state eventually. **(b)** Time series for one randomly chosen community, community 6. The pulse perturbations lead the community to an alternative stable state in the absence of memory (top), while adding memory effects allows recovering the original state (bottom). **(c)** Community dissimilarity (Bray-Curtis) between the start and the end of the simulation for all ten communities and different memory levels. Without memory, the pulse perturbation changes the abundances of some of the species and leads to an alternative stable state (*i.e.*, non-zero dissimilarity between start and end). In contrast, all communities recover their pre-perturbation stable state in the presence of memory (*i.e.*, zero dissimilarity). **(d)** Dissimilarity to the initial stable state through time in community 6, for different memory strengths.

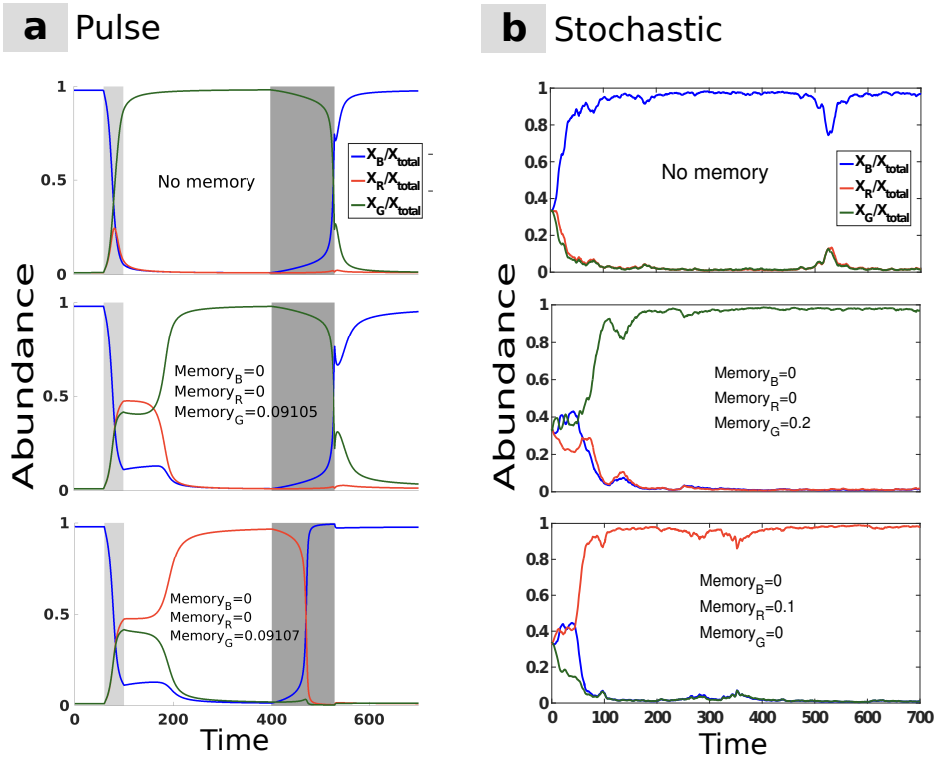

Fig S2. Role of memory in an incommensurate system. **(a)** The order derivative of X_G is a non-integer value, $0 < \mu_G < 1$, and the derivative order of X_B and X_R are integer, $\mu_B = \mu_R = 1$. Around a particular value of the order derivative of the green species ($\mu_G = 0.90895$), the system behaves differently after the first perturbation: for μ_G in the interval $]0.90895, 1]$, the green species will be dominant, while in the interval $]0, 0.90894]$ the red species will be dominant. **(b)** The growth rates follow the same Ornstein-Uhlenbeck process as in Fig 4. For the system without memory, the blue species is dominant. However, when imposing sufficient memory on the green or red species, they become dominant in the stable state.

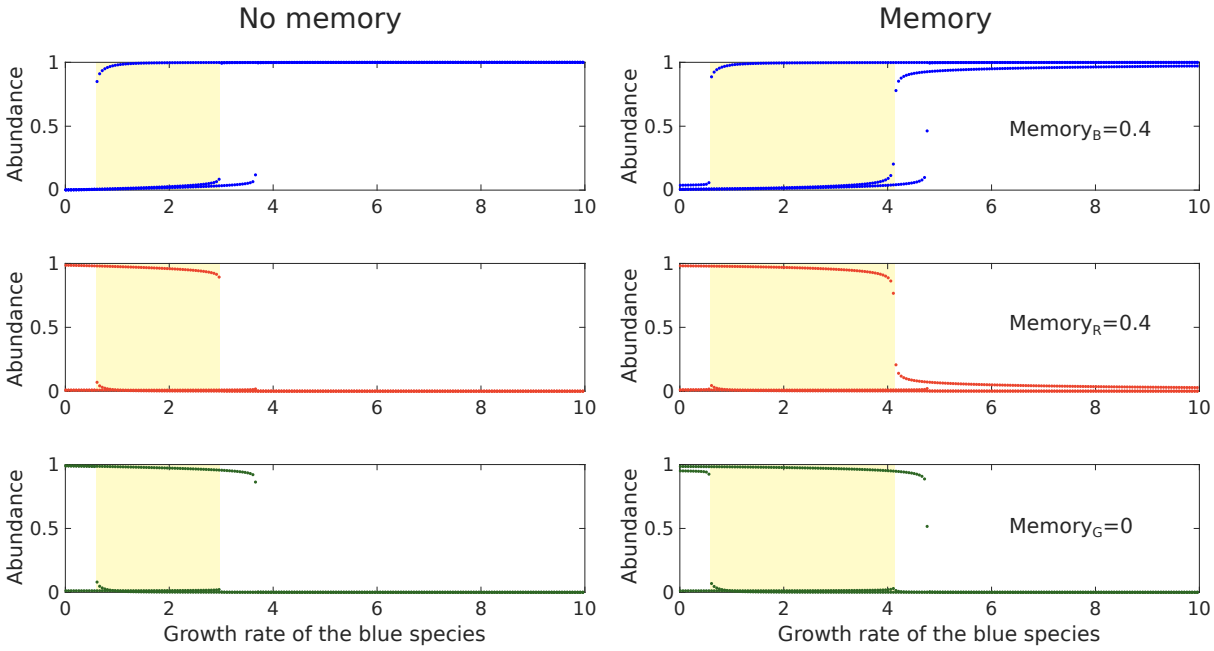

Fig S3. Memory broadens the model's multistable region. Bifurcation diagrams for the system shown in Fig 6, showing the relative abundance of the blue, red, and green species (from top to bottom) as a function of the blue species' growth rate for three different initial conditions (leading to three distinct curves per plot), in the absence (left) or presence (right) of memory. The yellow area shows the region of the parameter space that exhibits multistability, which is extended by the introduction of incommensurate memory (right).

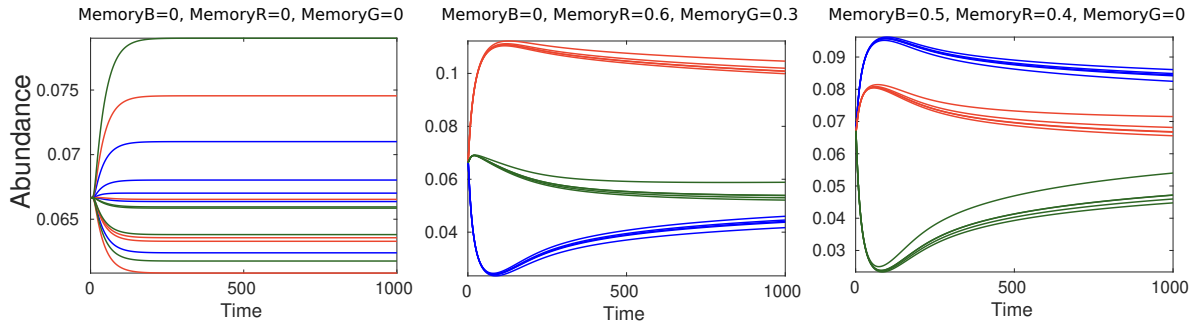

Fig S4. Groups of species can emerge from incommensurate memory. We consider here a 15-species community with equal interactions between species and identical initial abundances for all species, where species growth rates are drawn from $\mathcal{N}(1, 0.01)$. As expected, the species do not form groups in the absence of memory (left panel). When the species are randomly split into three groups (red, green, blue) with varying degrees of memory, species with a similar degree of memory tend to exhibit similar dynamics and group together due to their shared memory properties (middle panel). A switch to an alternative stable state can be triggered by changing the strength of memory effects (right panel).